Received: 2 March 2019 | Revised: 10 May 2019 | Accepted: 22 May 2019

DOI: 10.1111/gcb.14710

PRIMARY RESEARCH ARTICLE

Global Change Biology WILEY

Linking drought legacy effects across scales: From leaves to tree rings to ecosystems

Steven A. Kannenberg[1] | Kimberly A. Novick[2] | M. Ross Alexander[3] | Justin T. Maxwell[4,5] | David J. P. Moore[6] | Richard P. Phillips[7] | William R. L. Anderegg[1]

[1]School of Biological Sciences, University of Utah, Salt Lake City, Utah

[2]School of Public and Environmental Affairs, Indiana University, Bloomington, Indiana

[3]Midwest Dendro, LLC, Naperville, Illinois

[4]Department of Geography, Indiana University, Bloomington, Indiana

[5]Harvard Forest, Harvard University, Petersham, Massachusetts

[6]School of Natural Resources and the Environment, University of Arizona, Tucson, Arizona

[7]Department of Biology, Indiana University, Bloomington, Indiana

Correspondence
Steven A. Kannenberg, School of Biological Sciences, University of Utah, Salt Lake City, UT.
Email: s.kannenberg@utah.edu

Funding information
David and Lucile Packard Foundation; Indiana University Bloomington; Biological and Environmental Research, Grant/Award Number: DE-SC0016011; Division of Environmental Biology, Grant/Award Number: 1714972; National Institute of Food and Agriculture, Grant/Award Number: 2017-67013-26191 and 2018-67019-27850; Division of Emerging Frontiers, Grant/Award Number: 1802880; Department of Energy, Grant/Award Number: DE-SC0016011; NSF, Grant/Award Number: 1714972 and 1802880

Abstract

Severe drought can cause lagged effects on tree physiology that negatively impact forest functioning for years. These "drought legacy effects" have been widely documented in tree-ring records and could have important implications for our understanding of broader scale forest carbon cycling. However, legacy effects in tree-ring increments may be decoupled from ecosystem fluxes due to (a) postdrought alterations in carbon allocation patterns; (b) temporal asynchrony between radial growth and carbon uptake; and (c) dendrochronological sampling biases. In order to link legacy effects from tree rings to whole forests, we leveraged a rich dataset from a Midwestern US forest that was severely impacted by a drought in 2012. At this site, we compiled tree-ring records, leaf-level gas exchange, eddy flux measurements, dendrometer band data, and satellite remote sensing estimates of greenness and leaf area before, during, and after the 2012 drought. After accounting for the relative abundance of tree species in the stand, we estimate that legacy effects led to ~10% reductions in tree-ring width increments in the year following the severe drought. Despite this stand-scale reduction in radial growth, we found that leaf-level photosynthesis, gross primary productivity (GPP), and vegetation greenness were not suppressed in the year following the 2012 drought. Neither temporal asynchrony between radial growth and carbon uptake nor sampling biases could explain our observations of legacy effects in tree rings but not in GPP. Instead, elevated leaf-level photosynthesis co-occurred with reduced leaf area in early 2013, indicating that resources may have been allocated away from radial growth in conjunction with postdrought upregulation of photosynthesis and repair of canopy damage. Collectively, our results indicate that tree-ring legacy effects were not observed in other canopy processes, and that postdrought canopy allocation could be an important mechanism that decouples tree-ring signals from GPP.

KEYWORDS
carbon allocation, dendroecology, drought recovery, eddy covariance, remote sensing

1 | INTRODUCTION

Forests sequester 25% of annual anthropogenic carbon (C) emissions (Pan et al., 2011), thereby greatly slowing the pace of global climate change. However, forest responses to climate extremes such as drought remain one of the largest uncertainties in the C cycle (Reichstein et al., 2013) and are challenging to represent in many terrestrial biosphere models (Powell et al., 2013). This limited understanding of forest drought responses is particularly concerning given the projected increases in the frequency and severity of drought stress in the future (Cook, Ault, & Smerdon, 2015; Dai, 2013; Giorgi et al., 2011), which is likely to play an increasing role in determining forest C cycling dynamics (Clark et al., 2016). Therefore, understanding the processes that mediate the uncertainty in tree drought responses will be important for modeling the terrestrial carbon sink in the 21st century.

One such uncertainty lies in the ability of forests to recover from severe water deficits. In addition to impacting C uptake and growth during drought, the physiological changes trees undergo during water stress can also hinder recovery (Anderegg et al., 2013; Rowland et al., 2015; Trugman et al., 2018). Previous studies on these drought "legacy effects" have operated at contrasting scales, either (a) quantifying postdrought C uptake of whole ecosystems through terrestrial biosphere models, eddy covariance approaches, and remote sensing data products (e.g., Kolus et al., 2019, Schwalm et al., 2017, Wu et al., 2017); or (b) using tree-ring increments and forest inventories to quantify lags in individual tree growth after drought (e.g., Anderegg et al., 2015; Berdanier & Clark, 2016; Gazol, Camarero, Anderegg, & Vicente-Serrano, 2017; Camarero et al., 2018; Kannenberg, Maxwell, et al., 2019; Peltier, Fell, & Ogle, 2016). These two approaches can lead to apparently contrasting conclusions regarding the speed at which forests recover from drought stress—tree-ring and forest inventory-based studies often find multiyear lags in tree growth whereas findings at the ecosystem scale indicate much more rapid recovery of C uptake capacity.

Differences in the severity of legacy effects found in tree rings versus ecosystem C fluxes could be reconciled by considering that trees employ dynamic C allocation strategies that mediate tree recovery from drought stress. For example, altered nonstructural carbohydrate (NSC) dynamics (Richardson et al., 2013; Skomarkova et al., 2006), changes in canopy dynamics (Anderegg et al., 2016; Doughty et al., 2015), enhanced autotrophic respiration (Rowland et al., 2018), or increased root allocation (Doughty et al., 2014; Phillips et al., 2016) may be prioritized at the expense of stem growth both during and following drought. Therefore, the lagged effects of drought on C allocation patterns could result in reduced tree-ring increments despite a more rapid recovery of gross primary productivity (GPP). Thus, any C allocation away from stem growth postdrought could serve as a causal mechanism explaining the discrepancy between tree- versus ecosystem-level investigations of legacy effects.

Dynamic C allocation patterns postdrought are not the only mechanisms that could cause tree-ring increments to diverge from GPP. The temporal asynchrony between stem growth versus C uptake (Galiano et al., 2017; Mitchell, O'Grady, Tissue, Worledge, & Pinkard, 2014; Sala, Woodruff, & Meinzer, 2012) could also decouple legacy effects in tree rings from GPP, since radial growth tends to peak in late spring to early summer while C uptake occurs more uniformly throughout the growing season, at least in temperate and mesic forests (Čufar, Prislan, Luis, & Gričar, 2008; D'Orangeville et al., 2018; Delpierre, Berveiller, Granda, & Dufr, 2016). Given that the causal mechanisms for legacy effects—such as canopy loss, hydraulic damage, and NSC depletion (Bréda, Huc, Granier, & Dreyer, 2006; van der Molen et al., 2011)—should be most prevalent at the start of the postdrought growing season, it stands to reason that these mechanisms would affect tree ring formation to a greater extent than GPP. Additionally, standard tree-ring sampling techniques (for dendroclimatology purposes) focus on canopy dominant trees that best capture climate variability—likely biasing growth responses (DeRose, Shaw, & Long, 2017; Fritts, 1976; Nehrbass-Ahles et al., 2014) and potentially exacerbating the magnitude of legacy effects. Given these limitations, testing how tree-ring data can inform our understanding of whole forest functioning is seen as a crucial research frontier necessary to properly forecast the impacts of climate change on forest resources (Babst et al., 2018; Evans et al., 2017).

The impacts of these factors are likely highly variable across species and plant functional types. Thus, determining the mechanisms that underlie tree ring-detected legacy effects is therefore an important step for modeling the impacts of drought on whole forests. For example, if postdrought declines in stem growth are simply a consequence of lagged reductions in GPP (e.g., Campioli et al., 2016, Teets et al., 2017, Xu et al., 2017), model development efforts to better simulate drought legacies should focus more on the physiological mechanisms of postdrought limitations to GPP, such as changes in canopy structure or xylem embolism. However, if dynamic C allocation patterns postdrought decouple stem growth from GPP (e.g., Mund et al., 2010, Rocha, Goulden, Dunn, & Wofsy, 2006), legacy effects detected by tree rings may not necessarily suggest an impact on carbon uptake, but rather reflect shifting allocation patterns whose carbon cycle impacts would then be more determined by the turnover times of these other carbon pools (e.g., foliage, fine roots). Thus, examining whether tree growth and C uptake are coupled postdrought is critical for understanding the long-term C storage potential of forest ecosystems.

An explicit comparison of legacy effects in tree rings versus whole ecosystem fluxes has yet to be attempted. Establishing this linkage would serve to blend knowledge from tree-ring studies with emerging approaches for detecting drought legacies at broad spatial scales. Thus, we sought to examine legacy effects in tree rings, leaf-level photosynthesis, whole forest fluxes, and remote sensing products, and to understand the factors that could decouple tree rings from other C fluxes in the year following a severe drought. To do this, we leveraged data at Morgan–Monroe State Forest in south-central Indiana, a Midwestern AmeriFlux site that experienced a severe drought in 2012. At this site, we amassed a dataset consisting of tree-ring chronologies, dendrometer bands, leaf-level photosynthesis, stand surveys, eddy flux data, and MODIS leaf area index (LAI) and normalized difference

vegetation index (NDVI). In addition, our tree-ring chronologies were collected in two ways: a standard dendroclimatological approach that prioritized large and canopy dominant trees and a plot-based sampling approach that included understory trees. We asked:

- Q1: To what degree are drought legacy effects in tree rings apparent in leaf, canopy, and whole forest dynamics?
- Q2: Do dynamic C allocation patterns, temporal asynchrony between tree growth and GPP, or sampling biases decouple legacy effects in tree rings from GPP?

2 | MATERIALS AND METHODS

2.1 | Site

Our study site is located within the footprint of the Morgan–Monroe State Forest AmeriFlux tower (MMSF) near Bloomington, IN (39°19′N, 86°25′W). This site is a mesic (mean annual precipitation = 1,032 mm) deciduous broadleaf forest where tree growth is strongly controlled by variation in water availability (Brzostek et al., 2014; Yi et al., 2019). The canopy is dominated by hardwood species such as *Acer saccharum*, *Liriodendron tulipifera*, and *Quercus* spp. Most canopy dominant trees at MMSF are c. 90 years old and the forest canopy is 27 m in height.

In 2012, this site experienced a severe drought event (Figure S1) whereby June–July precipitation was less than 10% of the long-term (1991–2017) mean and soil moisture decreased to 50%–60% of the long-term mean. This drought, which resulted in the seventh lowest growing season Palmer Drought Severity Index at that site since 1901 (Dai, Trenberth, & Qian, 2004), also affected much of the Midwestern United States and is considered one of the "costliest … and most widespread natural disasters in US history" (Mallya, Zhao, Song, Niyogi, & Govindaraju, 2013), which reduced soil moisture to unprecedented levels during the peak of the growing season (Roman et al., 2015). This drought was also unusual due to its early timing—soil volumetric water content was reduced below 20% between day of year (DOY) 171–245. The severity of the 2012 drought, in addition to the wealth of data being collected at MMSF during that period, provides an excellent test bed for assessing legacy effects at multiple scales.

2.2 | Species composition

In order to scale species-specific tree-ring responses to the whole forest, we compiled estimates of tower footprint species composition. To do so, three 1,256 m^2 circular plots were set up in 2014 within the footprint of the tower as per the methods of Dye et al. (2016). Within these plots, the diameter at breast height of all stems >10 cm was measured and scaled to basal area (m^2/ha). Species composition was quantified as the percentage of total plot basal area occupied by each species and is used to scale up tree-level responses to the entire stand. However, *Carya ovata* was not present in these plots. Thus, we used basal area estimates for this species that were derived from our dendrometer band plots sampled in 2012 (see below). Species composition derived from our plots is consistent with previous estimates (Schmid, Grimmond, Cropley, Offerle, & Su, 2000).

2.3 | Tree-ring sampling

For the standard sampling approach (Fritts, 1976; Stokes & Smiley, 1999), tree-ring records were collected in 2016 for five of the most dominant species (by basal area) within the tower footprint. In this approach, trees were chosen to maximize the climate signal, meaning that all sampled trees were large, canopy dominant, mostly located on south-facing slopes, and had no visible damage or abnormalities. At least nine trees per species (Table 1) were sampled twice on opposite sides, parallel to the slope, with a 5 mm diameter increment borer at breast height. For our plot-based sampling approach (conducted in 2014), we sampled all trees across all canopy strata >20 cm in diameter in each of our plots (described above) in a similar manner as our standard sampling approach. As a result of this approach, many younger trees were cored that were not captured in our standard sampling approach, although we still cored many of the older trees in the stand (Table 1). This sampling approach resulted in coring mostly codominant and intermediate canopy classes, although some dominant and suppressed trees were also sampled (Table S1). The four most common species (*A. saccharum*, *L. tulipifera*, *Quercus alba*, and *Sassafras albidum*) were used for comparison with trees collected using the standard sampling approach. *C. ovata* was not present in

Sampling	Species	%BAI	#Cores	Mean DBH (cm)	Mean age (years)
Standard	*Acer saccharum*	0.271	10	45.2 ± 2.5	86 ± 1.9
Standard	*Carya ovata*	0.010	10	50.0 ± 1.8	106 ± 1.5
Standard	*Liriodendron tulipifera*	0.203	10	56.6 ± 3.8	69 ± 1.3
Standard	*Quercus alba*	0.155	9	37.1 ± 1.5	72 ± 1.6
Standard	*Sassafras albidum*	0.039	9	76.0 ± 2.5	88 ± 1.6
Plot-based	*A. saccharum*	0.271	26	30.1 ± 1.0	92 ± 0.7
Plot-based	*L. tulipifera*	0.203	9	57.8 ± 4.5	89 ± 2.8
Plot-based	*Q. alba*	0.155	7	55.7 ± 1.3	104 ± 0.7
Plot-based	*S. albidum*	0.039	7	24.1 ± 1.6	40 ± 0.9

TABLE 1 All species that were sampled (two cores per tree) with our standard and plot-based sampling approaches. % basal area index (BAI) indicates the proportion of total stand basal area for that species, as quantified by plot-based stand surveys. Thus, both sampling methodologies are paired with the same species composition estimates. Mean age is the mean length of the dated range for each species (cored at 1.3 m). Error for mean diameter at breast height (DBH) and mean age represents standard error

our plots, and thus, cores for this species were only collected via our standard sampling approach. Dendrochronological statistics are available in Table S2.

Following sampling, tree cores were dried, sanded, and measured on a measuring stage (Velmex, Bloomfield, NY) with the MEASURE J2X program (VoorTech Consulting, Holderness, NH) using standard dendrochronological techniques (Stokes & Smiley, 1999). Following measurement, cores were visually cross-dated (Yamaguchi, 1991), statistically checked using the program COFECHA (Holmes, 1983), and detrended using a two-thirds series length spline (Cook & Peters, 1981) with the R package *dplR* (Bunn, 2008). Cores from the same tree were averaged together using a biweight robust mean (Cook, 1985) and this tree-level chronology was used for all subsequent analysis.

2.4 | Eddy covariance measurements

The MMSF eddy covariance tower has been measuring carbon dioxide and water vapor fluxes since 1999 at a height of 46 m using a sonic anemometer (CSAT-3; Campbell Scientific, Logan, UT) and a closed-path infrared gas analyzer (LI-7000; LI-COR Biosciences, Lincoln, NE) that are calibrated weekly. Raw 10 Hz wind and gas concentration data are processed into hourly averaged fluxes of CO_2, which are then filtered to remove records collected during stable conditions (e.g., low friction velocity, see Dragoni et al., 2011). During nocturnal and dormant season periods, missing estimates of the net ecosystem exchange (NEE) are gap-filled using a temperature-dependent respiration function parameterized annually using acceptable observations. During the growing season, GPP is estimated as the difference between measured NEE and the temperature-driven ecosystem respiration (RE) estimates. When NEE, and thus GPP, estimates are missing, they are gap-filled using the RE model and a light-dependent function for GPP. As described in detail elsewhere, these gap-filling and partitioning approaches have been extensively tested and validated against other methodologies, and with multiple independent data sources (Ehman et al., 2002; Sulman, Roman, Scanlon, Wang, & Novick, 2016; van Gorsel et al., 2009).

2.5 | Leaf-level gas exchange measurements

Mid-day leaf-level C assimilation rates (*A*) were measured weekly at the top of the canopy during the growing seasons of 2011–2013 (Roman et al., 2015). These measurements were made on five sun-exposed leaves and five shaded leaves each of *A. saccharum*, *L. tulipifera*, *S. albidum*, *Q. alba*, and *Q. rubra*, using a LI-6400XT photosynthesis system (LI-COR Biosciences) set to 25°C leaf temperature and a flow rate of 500 μmol/s, while chamber photosynthetic photon flux density, CO_2, and water vapor concentrations were set to mirror ambient conditions.

2.6 | Dendrometer band data

Dendrometer bands have been installed on 330 trees within 34 plots (150 m^2) located in the tower footprint along transects ordinated NE, SE, and SW from the tower. Within each plot, all trees >10 cm in diameter at breast height (DBH) were banded, with care taken to avoid anomalous features of the bark. The majority of the plots were established before 2000, with approximately 25% of the plots established in 2012. Bands were measured approximately every 2 weeks during the growing season during the period of record. While the diameter of each banded tree is recorded at the beginning of the growing season, synchronizing the diameter increment information from the bands with the annual DBH snapshots introduces excessive noise linked largely to the sources of uncertainty in the tape-based measurements. Thus, for this analysis, all information on diameter provided by the dendrometer bands is referenced to a single tape-based measurement of DBH taken when the bands were installed.

Plots established in 2012 were excluded from our analysis (resulting in n = 250), as including these data biased our 2012 measurements due to bands "settling in" to the bark of the trees, though the inclusion of these data did not alter our results. Growth rates (in mm per day) were quantified as the change in tree radius between each sampling point, while the DOY of that growth rate was considered to be the midway point between samplings.

2.7 | Remote sensing products

We extracted MODIS LAI (MCD15A2H) and NDVI (MOD13Q1) using the *MODISTools* package in R (Tuck et al., 2014), which provides a convenient interface for the MODIS Land Products web service (https://modis.ornl.gov/data/modis_webservice.html). Eight-day window data (thus avoiding artifacts due to cloud cover) were extracted for MMSF site coordinates for 2000–2015 and binned by month for subsequent analysis.

2.8 | Drought and legacy effect quantification

Drought effects and legacy effects in tree rings were calculated via the method of Kannenberg, Maxwell, et al. (2019). For each tree-ring series, a linear model (mean correlation coefficient = 0.33) was created between detrended ring width increment (RWI) and annual May–September summed climatic water deficit (CWD, precipitation − potential evapotranspiration). Climate data products for MMSF were obtained from the CRU TS 3.24.01 dataset (Harris, Jones, Osborn, & Lister, 2014). These linear models were then used to predict what RWI should be (in the absence of legacy effects) given that growing season's CWD. Legacy effects were then quantified as the difference between observed and predicted RWI, multiplied by 100. Given that our detrending method results in an average RWI of 1, this quantification is analogous to an effect size. Drought effects in tree-ring increments were also quantified as effect sizes:

$$\text{Drought effect} = \left(\frac{\overline{\text{RWI}} - \text{RWI}_{2012}}{\overline{\text{RWI}}} \right) \times 100$$

where $\overline{\text{RWI}}$ represents the mean RWI across the entire tree-ring series and RWI_{2012} represents the RWI in 2012 of each cored tree.

Using our species composition estimates, we scaled species-specific tree-ring responses to the stand level using a weighted mean approach:

$$RWI_{stand} = \frac{\sum \frac{RWI_{2012,2013}}{\text{Species sum}}}{\sum \frac{RWI_{Normal}}{\text{Species sum}}} \times 100$$

where RWI_{stand} represents the stand-weighted drought effect or legacy effect, $RWI_{2012,\ 2013}$ represents each individual tree-ring increment in 2012 or 2013 multiplied by that species' % basal area, RWI_{Normal} is the average tree-ring increment in all other years multiplied by that species' % basal area, and species sum is the total % species composition represented by our tree-ring series (67.8%). With this scaling exercise, it was our intention to provide a metric of legacy effect size in tree rings that would be more directly comparable with the spatial scale of eddy covariance and remote sensing data products. However, there exists the potential for this scaling to be biased if there are differences in legacy effect magnitude across tree size classes. To determine if legacy effects vary with tree size, we constructed linear models between individual tree diameter and legacy effect size in 2013. We detected no significant correlations ($p = 0.73$), and thus did not include tree diameter in our scaling from individual trees to the whole stand.

Drought effects and legacy effects in leaf-level gas exchange were quantified as an effect size of photosynthesis during the peak 2012 drought period (DOY 171–245), late 2012 following the cessation of the drought (DOY 246–287), and early 2013 (DOY 135–200). These individual measurements from 2012 and 2013 were converted into effect sizes (as above) by comparing with the mean of all measurements for a particular species during nondrought conditions. These nondrought periods included any periods in 2011 and 2012 where daily average volumetric water content was above 20% including early 2012 (DOY 117–170) and most of 2011 until a mild late season drought starting on DOY 200.

We quantified legacy effects in GPP with four methods: (a) comparing ecosystem fluxes in 2013 to historical (nondrought, i.e., 2000–2011 and 2014–2017) means; (b) a multiple linear regression; (c) the light response curve model (and vapor pressure deficit function) commonly used to partition ecosystem fluxes into GPP (Lasslop et al., 2010) parameterized via the standard approach; and (d) the same light response curve approach, but parameterized only with nondrought data. Our multiple linear regression approach initially considered all primary drivers of GPP measured by the flux tower (soil water content, incoming shortwave radiation, vapor pressure deficit, soil temperature, and air temperature), which were standardized by converting each hourly value into a *z*-score. We then removed variables that were highly collinear (variance inflation factor >5) and performed model selection on the remaining variables using Akaike's information criterion. This procedure resulted in the removal of air temperature from our multiple regression model due to high collinearity with vapor pressure deficit and soil temperature. Its removal did not impact the predictive ability of the final model. While soil moisture and vapor pressure deficit are correlated at long timescales (weekly to monthly), they are largely decoupled over the hourly timescales at which flux tower data are collected (Novick et al., 2016).

For the light response curve approaches, we fit all parameters using the nonlinear least squares function *nls* in base R for 5-day windows across the entire flux data record. We chose parameter estimation starting points and culled anomalous parameter estimates according to the protocol of Lasslop et al. (2010). We used these parameters to predict GPP in two ways in order to circumvent potential biases when calculating legacy effects. First, we used parameter estimates for each 5-day window to predict GPP within that window—the standard approach of Lasslop et al. (2010). This method had the benefit of being parameterized for a given season's meteorological conditions and forest dynamics. However, legacy effects could be caused by leaf-level suppression of photosynthesis, meaning that our parameterization method would potentially incorporate such effects, thus causing our prediction of what GPP should be (in the absence of legacy effects) to actually include those legacy effects. Therefore, we also used our light response curve model when parameterized with data from all years other than 2012 or 2013 (i.e., 2000–2011 and 2014–2017). Thus, this method would capture basic forest phenology yet bypass the limitation described above. All of our methods were only applied to DOY 100–300 in order to capture the relevant phenological phases of the growing season in this forest.

2.9 | Data analysis

Peaks in radial growth and GPP were quantified by applying the nonparametric, local regression smoothing function *loess* in base R (with a 25% span) to our growing season radial growth and GPP data. The peaks for radial growth and GPP were considered as the DOY at the maximum value of these smoothed curves. Our results were similar when including all sampled trees on the dendrometer band plots or considering only the species that we cored (Table S3). Additionally, the timing of peak radial growth was consistent across species (Table S3). Therefore, we have included all sampled tree species for this analysis. Dendrometer band measurements outside of DOY 100–300 were excluded to be consistent with our analysis of flux tower data.

One-way *t* tests were conducted to assess the statistical significance of drought and legacy effects in tree rings, with Tukey tests for between species pairwise comparisons, while independent two-group *t* tests were used to assess differences between sampling approaches within individual species. Differences in MODIS LAI and NDVI in a given month between nondrought years, 2012 and 2013, were also assessed using Tukey pairwise comparisons.

3 | RESULTS

3.1 | Differences between tree-ring sampling methodologies

Our two sampling approaches yielded similar results, as most species' drought effects (Figure 1a) and legacy effects (Figure 1b) were

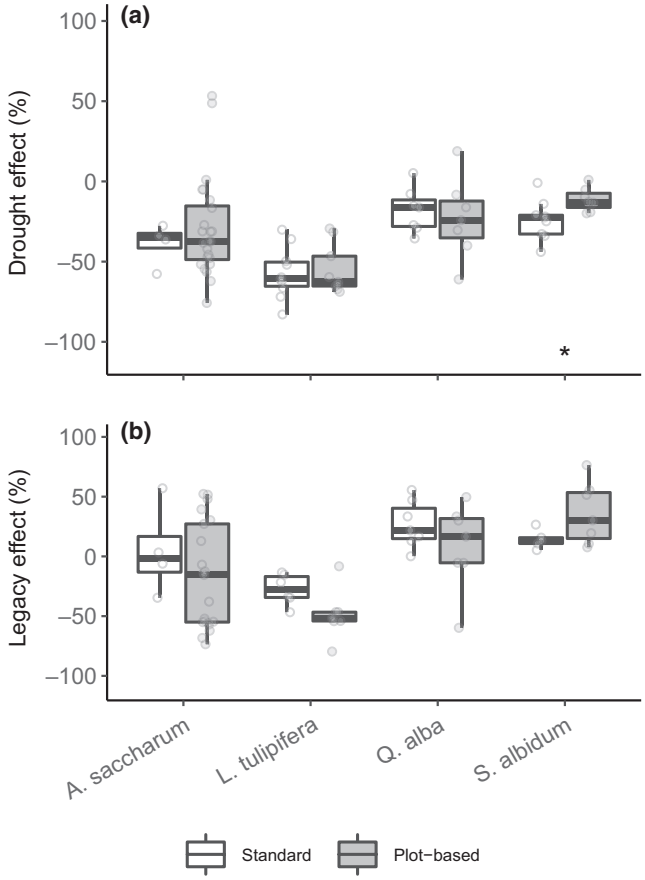

FIGURE 1 Drought effects (a) and legacy effects (b) in tree-ring increments quantified with our standard versus plot-based sampling approaches. Drought effects were calculated as effect sizes of the difference between 2012 ring width increment (RWI) relative to mean RWI, and legacy effects were calculated as effect sizes of predicted minus observed ring widths relative to mean RWI. Asterisks indicate statistical significance between sampling approaches within a species ($\alpha = 0.05$). Outliers have been excluded from the figure but are present in all statistical analyses

statistically indistinguishable when using a plot-based sampling versus standard sampling approach. The one exception was *S. albidum*, which showed slightly smaller drought effects when sampled via the plot-based approach ($p = 0.01$). Thus, we pooled our tree-ring series for all subsequent analysis.

3.2 | Tree-ring responses to drought

All species significantly reduced tree-ring increments in response to the 2012 drought (Figure 2a, $p < 0.001$). The size of this drought effect was statistically similar for four of five species, with reductions in RWI between 17% and 26%. The drought had a much larger effect on *L. tulipifera*, however, with observed reductions in RWI averaging 56%.

Ring width increment was also impacted in 2013, as every species except *A. saccharum* had tree-ring increments that deviated from normal (Figure 2b). However, this effect was actually positive for *C. ovata*, *Q. alba*, and *S. albidum*, causing anomalies from predicted RWI of 32%, 18%, and 27%, respectively. In contrast, RWI was suppressed in 2013 by 26% for *L. tulipifera*. These individual species responses, when scaled to the stand level using species composition data, resulted in a weighted RWI reduction of 36% in 2012 and a legacy effect in RWI of 10% in 2013 (Figure 2c).

3.3 | Leaf-level photosynthesis

Drought decreased leaf-level photosynthesis by between 23% and 30% for three of five species (Figure 3, $p < 0.01$ for all species). The other two species, *Q. alba* and *Q. rubra*, were unaffected by the drought and did not reduce photosynthesis as compared to nondrought periods. Following the cessation of the drought, photosynthesis recovered quickly and only remained suppressed in *L. tulipifera* ($p = 0.05$). Photosynthesis was also not reduced in early 2013 (DOY 135–200), and in fact was significantly elevated in all species ($p < 0.01$ for all species). However, no pairwise differences between species could be detected for drought effects, late 2012 legacy effects, or early 2013 legacy effects.

3.4 | Gross primary productivity

In general, we found high agreement between all methods for predicting GPP (Figure S2), although our standard light response curve approach was best able to replicate nighttime partitioned GPP ($r^2 = 0.81$). Seasonal trends in GPP largely mirrored those in leaf-level photosynthesis. During "normal years" (i.e., years in the flux record besides 2012–2013), MMSF averaged an annual GPP sum of 1,358 μmol CO_2/m^2 across DOY 100–300 (Figure 4a). In 2012, GPP from DOY 100–300 was suppressed by 13.1% as compared to historical mean fluxes, though this reduction in GPP was 31.4% when only considering days when the drought peaked (DOY 171–245).

In order to separate responses to interannual variability in weather from potential legacy effects, we predicted what GPP should be (in the absence of legacy effects) using four different approaches. For the first approach, GPP recovered in 2013, even surpassing mean GPP from DOY 100–300 at 1,401 μmol CO_2/m^2. The second approach, a multiple linear regression, underpredicted the reduction in GPP due to drought (Figure 4b, a 9.0% reduction in GPP during DOY 171–245), but GPP predicted by this model fully recovered in 2013 and tracked historical mean fluxes over the growing season. Our standard light response curve approach (with proper parameterization) largely agreed with our first approach, predicting a 8.7% decrease in 2012 GPP during DOY 100–300 and a 30.1% decline during the peak of the drought (DOY 171–245), while GPP rapidly recovered in 2013 (Figure 4c). Our average parameter light response curve approach, however, failed to capture any drought effects in 2012, which is not surprising given that it is fit using nondrought parameters (Figure 4d).

We then sought to quantify the magnitude of legacy effects by subtracting nighttime partitioned GPP from predicted GPP, an approach analogous to the "predicted minus observed" calculation of legacy effects in tree rings. Using the standard light response curve

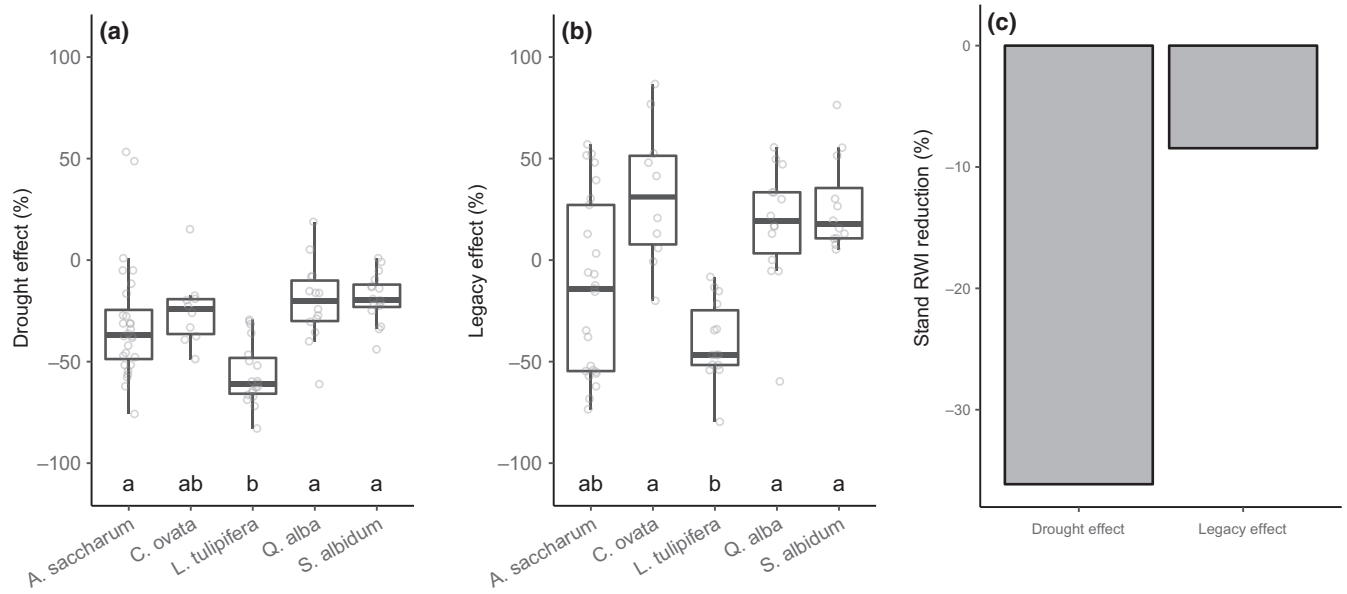

FIGURE 2 Drought effects (a) and legacy effects (b) across all species and sampling approaches at the Morgan–Monroe State Forest AmeriFlux tower. Drought effects were calculated as effect sizes of the difference between 2012 ring width increment (RWI) relative to mean RWI, and legacy effects were calculated as effect sizes of predicted minus observed ring widths relative to mean RWI. Lettering represents statistical significance between species via pairwise comparisons. (c) Stand-scale (weighted by species composition) drought effects and legacy effects. Outliers have been excluded from the figure but are present in all statistical analyses

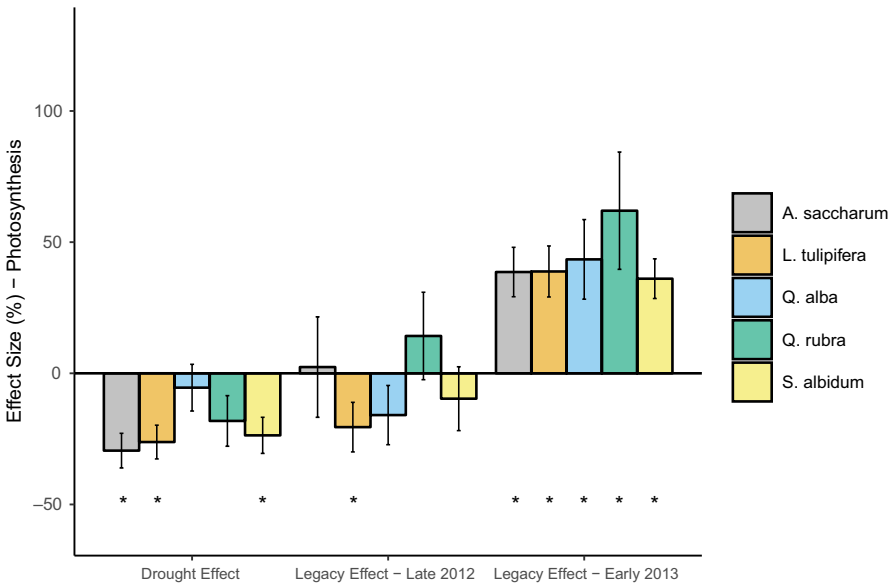

FIGURE 3 Effect sizes of leaf-level photosynthesis during the drought ("Drought Effect," day of year [DOY] 171–245), during 2012 once the drought ceased ("Legacy Effect—Late 2012," DOY 246–287), and early in the spring of 2013 ("Legacy Effect—Early 2013," DOY 135–200). Asterisks represent statistical significance from zero ($p < 0.05$). No significant pairwise comparisons between species within a given time period were detected. Error bars represent ±*SE*

method, the summed growing season legacy effect in GPP was 33.2 µmol CO_2/m^2 and predicted fluxes did not deviate at any point during DOY 100–300 (Figure 5). Likewise, GPP legacy effects calculated from our multiple regression approach and average parameter light response curve approaches were similarly small and positive (137.1 and 37.7 µmol CO_2/m^2, respectively). Thus, all four of our methods indicate that GPP was actually slightly higher in 2013 than we would predict, but the magnitude of this effect was relatively minor and nonsignificant throughout the season.

3.5 | Timing of radial growth versus GPP

In general, radial growth (as measured by dendrometer bands) followed the same temporal pattern as GPP. In 2012, radial growth (Figure 6c) peaked on DOY 144 and declined sharply as the drought commenced, whereas GPP peaked at DOY 155 (Figure 6a). In 2013, radial growth (Figure 6d) and GPP (Figure 6b) tracked each other closely, with radial growth peaking at DOY 174 and GPP peaking at DOY 177. These were fairly average peaks, as in all other

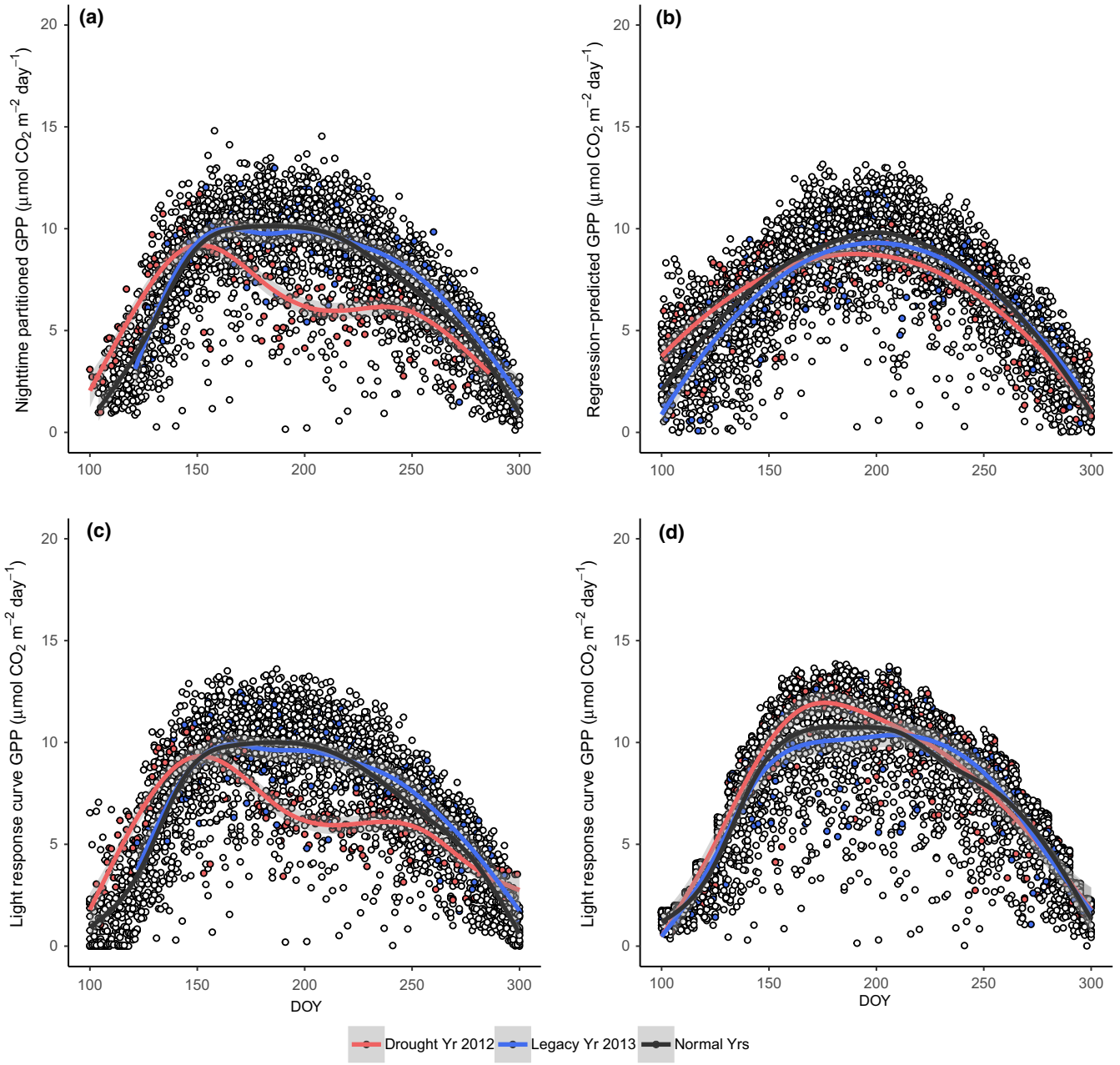

FIGURE 4 Seasonal cycles of daily gross primary productivity (GPP) during the 2012 drought, the 2013 "legacy effect" year, and all other years within the flux record. (a) GPP partitioned using the nighttime approach. (b) GPP predicted with our multiple regression approach. (c, d) GPP predicted with a light response curve using standard parameterization and average parameter values, respectively. Each point represents summed daily GPP and colored lines represent the smoothed trend line of these data

years combined radial growth was highest at DOY 156 and GPP was highest at DOY 185.

3.6 | Remote sensing products

MODIS-derived NDVI and LAI were fairly consistent across the growing season during nondrought years. In 2012, however, drought significantly suppressed NDVI in July (Figure 7a, $p = 0.01$) and continued to be moderately significantly suppressed in August (Figure 7a, $p = 0.07$). In 2013, however, NDVI fully recovered and remained in line with historical means throughout the year. LAI was not affected by the drought in any months of the growing season yet was reduced in May 2013 (Figure 7b, $p = 0.04$) and moderately significantly decreased in June 2013 (Figure 7b, $p = 0.06$).

4 | DISCUSSION

Despite increasing recognition of the importance of legacy effects on tree growth (Anderegg et al., 2015; Gazol et al., 2017; Camarero et al., 2018; Kannenberg, Maxwell, et al., 2019; Peltier et al., 2016),

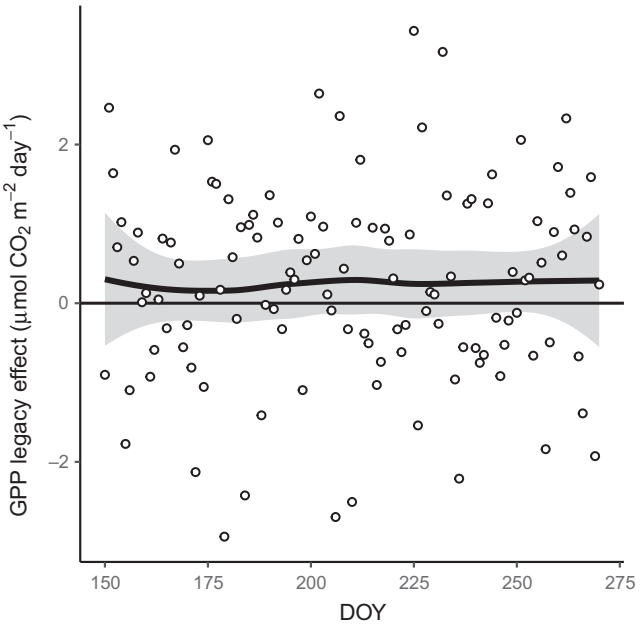

FIGURE 5 Legacy effects in gross primary productivity (GPP) in 2013 during the peak of the growing season (day of year [DOY] 150–270), quantified as nighttime partitioned GPP minus GPP predicted with our standard light response curve approach. Legacy effects in GPP were not significantly different from zero at any point during the growing season. Each point represents summed daily GPP, and shaded gray areas represent the 95% confidence interval around the smoothed trend line

we lack a mechanistic understanding of the ecosystem consequences of this phenomenon. Here, we found that while drought may impart legacy effects in radial stem growth, other aspects of ecosystem C cycling were not suppressed. Moreover, we found lagged effects on canopy-scale LAI that were compensated for by increases in leaf-level photosynthesis—resulting in no net change in GPP. Thus, our results highlight that the ecosystem consequences of legacy effects may hinge on the C allocation strategies of the dominant trees, especially if C is allocated toward pools with shorter turnover times.

4.1 | Tree-ring responses to drought

We found legacy effects in tree rings to be highly species specific, but the stand-weighted size (~10%) was in line with other investigations (Anderegg et al., 2015; Gazol et al., 2017; Camarero et al., 2018; Kannenberg, Maxwell, et al., 2019). In accordance with other recent studies (Elliott, Miniat, Pederson, & Laseter, 2015; Kannenberg, Maxwell, et al., 2019; Yi et al., 2019), we found species with diffuse porous wood anatomy (*A. saccharum* and *L. tulipifera*) to be more sensitive to drought and have larger legacy effects. In the context of the 2012 drought, which occurred later relative to the start of the growing season, wood anatomy could play a large role in dictating drought responses and recovery. Since ring porous species produce large vessels early in the season that are responsible for most of that ring's hydraulic conductivity (Zimmerman, 1983), a late season drought should have larger effects on diffuse porous species (which produce smaller vessels throughout the entire growing season). Subsequently, it should be easier for ring porous species to recover as restoring hydraulic conductivity can be facilitated by creating new, large, earlywood vessels at the start of the next growing season. While research into the factors that give rise to variation in legacy effects is still sparse, the species specificity in drought effects and legacy effects highlights the value of our scaling approach. A large challenge in forest research is linking individual tree responses to stand-level dynamics (Clark et al., 2016), and indeed if we did not scale our tree-ring responses using species composition data, we would have falsely concluded that legacy effects in RWI did not occur at the stand scale in response to the 2012 drought.

Surprisingly, some species actually had positive legacy effects (larger than expected postdrought RWI). This interesting finding could reflect a number of demographic and biogeochemical changes postdrought, such as release from competition (though no drought-induced mortality was observed at MMSF, Lloret, Escudero, Iriondo, Martínez-Vilalta, & Valladares, 2012; Pretzsch, Schütze, & Uhl, 2013), hydraulic lift from neighboring deep-rooted trees (Brooks, Meinzer, Coulombe, & Gregg, 2002; Landsberg & Waring, 2016; Oliveira, Dawson, Burgess, & Nepstad, 2005), or increases in nutrient availability (Gessler, Schaub, & McDowell, 2016; Schimel, Balser, & Wallenstein, 2007; van der Molen et al., 2011). However, the basal area represented by the species with positive legacy effects was small, and thus, the species with negative legacy effects (*A. saccharum* and *L. tulipifera*) that dominated the total basal area of the stand were responsible for the observed stand-scale reduction in tree-ring increment postdrought.

While uncertainty introduced due to the types of trees that are selecting for coring can be substantial (Alexander, Rollinson, Babst, Trouet, & Moore, 2018; Dye et al., 2018), we do not believe that sampling methodology significantly altered our conclusions. Uncertainty from tree selection occurs partially because tree susceptibility to drought has been observed in some cases to be highest in large, old trees (Bennett, McDowell, Allen, & Anderson-Teixeira, 2015; Nepstad, Tohver, Ray, Moutinho, & Cardinot, 2007; Phillips et al., 2010), which could increase the size of legacy effects in trees that are typically selected via standard dendrochronological sampling approaches (Klesse et al., 2018). However, these large trees many times comprise a disproportionate amount of biomass in older forests (Dye et al., 2018; Lutz et al., 2018), thus making the responses of these trees highly consequential for overall forest C cycling. Given that we did not observe any relationship between tree diameter and legacy effect size, nor did we see large differences between our standard and plot-based approaches, our results add to evidence suggesting that sampling bias introduces the most uncertainty when quantifying overall growth and biomass, not growth responses to short-term climate variability (Alexander et al., 2018; Nehrbass-Ahles et al., 2014).

4.2 | Recovery of leaf-level photosynthesis

Legacy effects in tree rings were not associated with widespread declines in leaf-level photosynthesis—either immediately after the

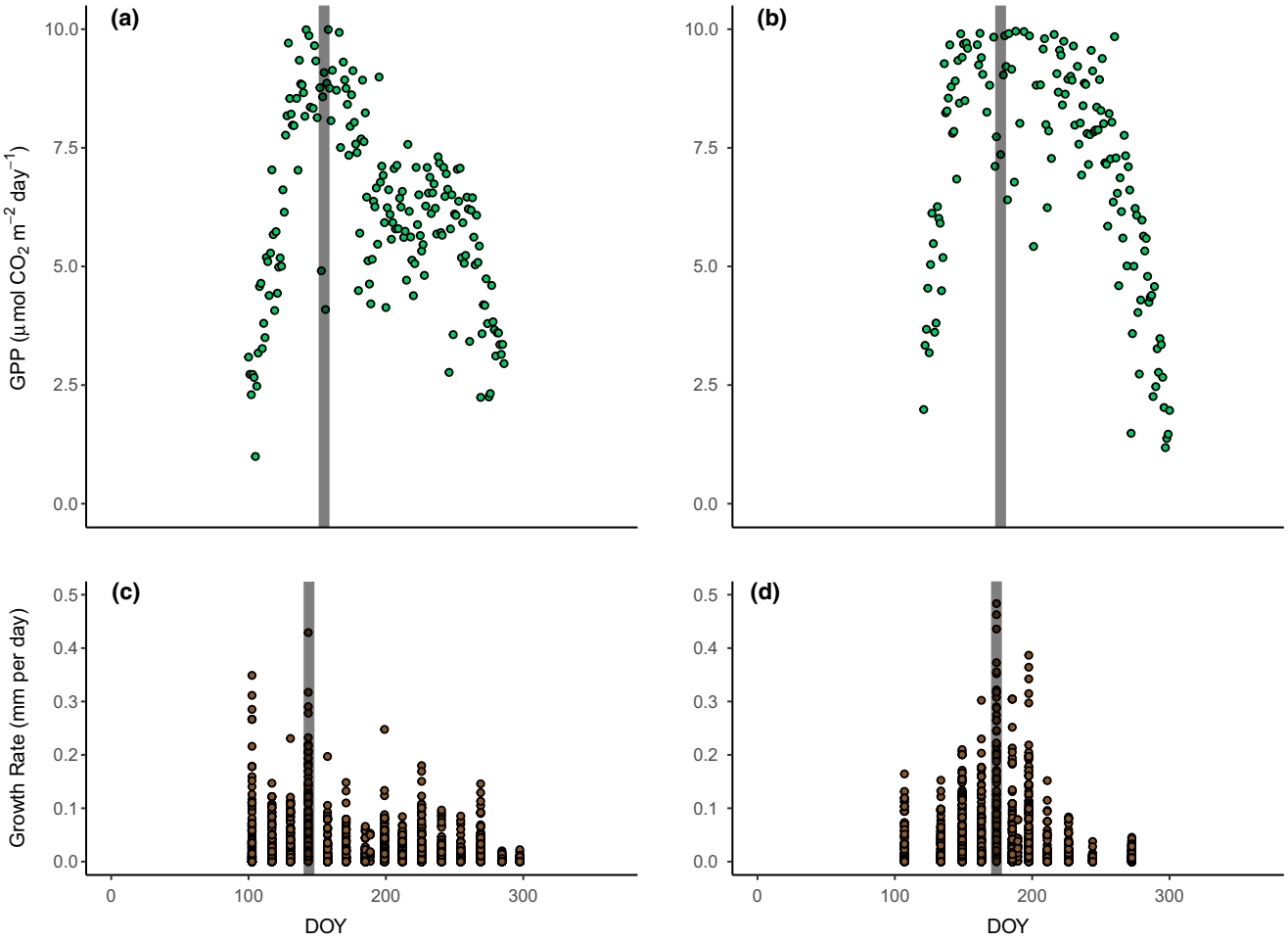

FIGURE 6 Growing season gross primary productivity (GPP) in 2012 (a) and 2013 (b), and radial growth from dendrometer band data in 2012 (c) and 2013 (d). Each point in (a) and (b) represents a summed daily flux of GPP, while each data point in (c) and (d) represents the growth rate of one measured tree at that time point. Vertical gray bars represent the peak of each smoothed time series

FIGURE 7 MODIS-derived normalized difference vegetation index (NDVI) (a) and leaf area index (LAI) (b) for May–September during the 2012 drought, the 2013 "legacy effect" year, and all other years within 2000–2015. All data are binned by month and error bars represent ±*SE*

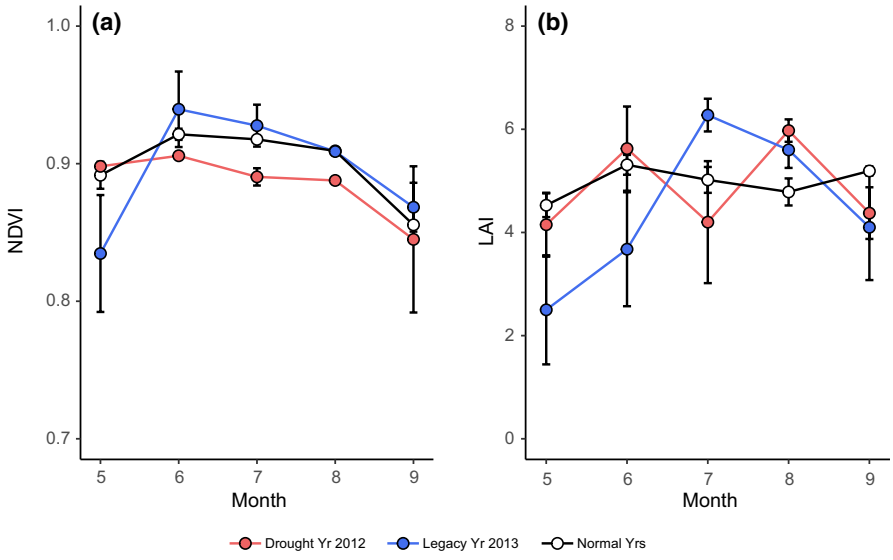

drought ceased in 2012 or in early 2013. In fact, photosynthesis was significantly elevated in early 2013 for all species. The rapid recovery of photosynthesis is perhaps surprising given that photosynthesis has often been observed to take weeks to recover in greenhouse experiments (Gallé, Haldimann, & Feller, 2007; Kannenberg, Novick, & Phillips, 2019). However, these experimental droughts are likely more

severe than those in forests, potentially introducing biochemical (instead of stomatal) limitations on photosynthesis (Flexas & Medrano, 2002). In addition, it is worth noting that *L. tulipifera*—the species with the largest legacy effects in tree rings—was the only species to experience reduced photosynthesis following the 2012 drought. These results confirm previous work indicating that numerous aspects of *L. tulipifera* physiology are highly sensitive to drought, including RWI (Kannenberg, Maxwell, et al., 2019), radial growth (Brzostek et al., 2014), sap flux (Yi, Dragoni, Phillips, Roman, & Novick, 2017), and photosynthesis (Roman et al., 2015). These results potentially highlight fundamental trade-offs between maintaining C supply and allocating that C to various sinks. While it is well known that drought induces significant alterations in C allocation (Bréda et al., 2006; van der Molen et al., 2011), the species-specific interactions between legacy effects, C supply, and various C sinks remain unresolved.

4.3 | Drought effects and legacy effects in GPP

Previous attempts to uncover legacy effects in larger scale C cycle processes have been limited by their large spatial and temporal breadth (Schwalm et al., 2017; Wu et al., 2017), while other studies linking tree rings to GPP have not examined this question in the context of environmental stress (Mund et al., 2010; Ouimette et al., 2018; Rocha et al., 2006; Rollinson et al., 2017). Thus, we lack a comprehensive understanding of how legacy effects affect the C cycle. We used four different approaches to estimate postdrought legacy effects on GPP. All four of these methods—comparisons to historical mean fluxes, a multiple regression approach, and a light response curve parameterized in two different ways—pointed to the same conclusion: legacy effects in tree rings are decoupled from ecosystem C uptake. The standard light response curve approach predicted drought-induced declines in GPP in 2012 that were comparable with nighttime partitioned values. The fact that the light response curve approach that used parameter values averaged across all years (instead of the usual year by year method) failed to replicate drought-induced declines in GPP likely indicates that the effects of drought were factored out during the parameterization of the model. This is unsurprising as the key model parameters are related to light utilization efficiency and maximum carbon uptake at light saturation (Lasslop et al., 2010), which would both be suppressed during drought due to stomatal closure or biochemical limitation of photosynthesis (Stocker et al., 2018). Therefore, using nondrought values of these parameters to estimate GPP during drought would not capture any drought response. Likewise, the multiple regression approach predicted much smaller drought-induced suppression of GPP. This is likely due to the fact that only one model predictor—soil moisture (and to a lesser extent, vapor pressure deficit)—was anomalously low during the 2012 drought. Since the other model parameters (incoming shortwave radiation and soil temperature) were fairly average in 2012, it is unsurprising that a nonmechanistic multiple regression approach could not simulate the severity of the drought.

Overall, the standard light response curve approach best approximated our nighttime partitioned data. Therefore, we feel that the (a) comparison to historical mean fluxes and (b) the standard light response curve approaches are most justified. With these methods, we could not detect any significant legacy effects in GPP. Most notably, we failed to observe legacy effects early in the growing season when drought-induced damage—such as NSC depletion, hydraulic damage, or canopy dieback—would be expected to be most significant. In sum, we did not find evidence that legacy effects in tree ring scaled to affect GPP, consistent with our leaf-level observations of photosynthesis.

4.4 | NDVI and LAI

We found that the 2012 drought suppressed NDVI at MMSF yet returned to historical averages once the drought ceased and continued to not deviate from the norm in 2013. Tree rings have been found to be more sensitive to drought when compared to NDVI (Gazol et al., 2018), possibly due to an underestimation of drought impacts that is inherent in many remotely sensed data products (Stocker et al., 2019). Thus, tree-ring widths and remotely sensed data products may be poorly correlated with each other in some ecosystems (Seftigen, Frank, Björklund, Babst, & Poulter, 2018). Our results build on these findings, further suggesting that NDVI during drought is less affected than tree-ring increment and that legacy effects that are apparent in tree rings are not present in NDVI. However, we did find evidence for lagged impacts of drought on LAI, as LAI remained suppressed in May and June of 2013. This suggests that some of the physiological effects of the 2012 drought (e.g., hydraulic damage, NSC depletion, bud production) persisted and affected leaf out in the following spring. Canopy damage and delayed leaf out has been suggested as one potential mechanism underlying legacy effects in tree rings due to reduced photosynthetic capacity or preferential allocation to the canopy (Anderegg et al., 2013, 2015; Doughty et al., 2015). However, the decreases in LAI we observed were not linked to reductions in GPP and were actually associated with significant increases in photosynthesis at the leaf scale. Thus, increased photosynthetic rates compensated for canopy loss, highlighting that the interaction between leaf area and photosynthetic rates is a dynamic process in the context of drought stress.

4.5 | Integrating cross-scale measurements to gain mechanistic understanding of legacy effects

We identified three potential mechanisms that could decouple legacy effects in tree rings from GPP. First, if we assume that drought-induced damage is more prevalent in the early season following a drought, we would expect that radial growth occurring sooner than peak canopy C uptake could cause legacy effects in RWI but not in ecosystem fluxes. However, this explanation is unlikely, as peak radial growth and peak GPP occurred within a 4-day window in 2013. Second, standard tree-ring approaches could bias tree ring collection in favor of trees that show high climate sensitivity—thus exacerbating the size of legacy effects. This explanation is also unlikely, as species' legacy effects using a standard approach were

mostly indistinguishable from those estimated using a plot-based approach. Finally, competing C sinks could be prioritized over radial growth postdrought, thus causing reductions in RWI despite recovery of ecosystem C uptake. Our results most strongly support this hypothesis, as LAI was reduced early in the 2013 growing season. Despite this reduction in leaf area, GPP was maintained due to an increase in leaf-level photosynthesis. This increase in photosynthesis could be due to increased light availability (due to reduced LAI), postdrought nutrient pulses (Schimel et al., 2007), or active allocation of resources to upregulate photosynthesis and rebuild the canopy (Doughty et al., 2015). It is also likely that other C sinks such as NSCs, fine roots, and repair of other drought-induced damage could also be prioritized, but more research is needed to explicitly test these mechanisms. Understanding the mechanistic underpinnings of these drought-induced shifts in allocation, and the timescales over which these changes persist, will be crucial for improving how vegetation models represent forest C cycling.

The extent to which our results are generalizable to other sites is yet unknown. MMSF is a fairly mesic forest and tree-ring increments are not typically highly sensitive to water availability (Maxwell, Harley, & Robeson, 2016). In more xeric forests, the responses of understory versus canopy dominant trees may diverge to a greater extent due to (a) larger trees being more affected by drought (Bennett et al., 2015; Nepstad et al., 2007; though see Colangelo et al., 2017; Stephenson, Das, Ampersee, Bulaon, & Yee, 2019 for recent counterexamples); or (b) smaller trees having less access to soil water and smaller NSC stores (Sala et al., 2012). The site and context specificity of tree-ring sampling biases would be a fruitful avenue of research and assist future efforts at collecting ecologically relevant tree-ring chronologies.

5 | CONCLUSIONS

The C storage capacity of forests is a crucial process that sustains myriad ecosystem services and serves as a negative feedback on climate change. However, the strength of this feedback in the future is uncertain, in part due to the unknown ability of these systems to recover from extreme climatic events. As the ability of forests to recover in the face of increasing water stress is likely to be paramount in determining the future terrestrial C sink, we need to be able to link our current understanding of legacy effects at the individual scale with whole forest processes (Babst et al., 2018; Clark et al., 2016; Evans et al., 2017). In an attempt to connect postdrought suppression of radial growth to ecosystem C uptake, we have found that legacy effects in tree-ring increment do not indicate reductions in leaf-level or ecosystem-level C cycling, and provide evidence that lagged canopy allocation is a potential mechanism for this decoupling. However, legacy effects in wood growth could still impact long-term C storage because C is being allocated away from wood toward pools with shorter turnover times. These results also have important implications for dendroecology, as we found tree rings at MMSF were poor proxies for ecosystem C uptake following drought stress. While drought—and its interactions with co-occurring stressors such as heat waves and pests—are seen as a major force shaping forest C cycling and demography (Bonan, 2008; Reichstein et al., 2013; Vose, Clark, Luce, & Patel-Weynand, 2016), it is crucial that we also understand how tree recovery affects whole ecosystems in order to properly forecast forest health in the face of global increases in aridity.

ACKNOWLEDGEMENTS

We would like to extend a special thanks to Tyler Roman for collecting leaf-level photosynthesis data, as well as Koong Yi for collecting some tree-ring data and Anna Trugman for assistance extracting remote sensing data. The authors are grateful for support from the Morgan–Monroe State Forest flux tower provided by the US Department of Energy through the AmeriFlux management project. SAK, KAN, JTM, and RPP also acknowledge support from the US Department of Agriculture National Institute of Food and Agriculture, Agricultural and Food Research Initiative Competitive Program #2017-67013-26191. Funding for tree-ring data collection was provided to JTM by the Indiana University Vice Provost of Research Faculty Research Program and additional tree-ring collection funding was provided to DJPM and MRA through the Department of Energy Regional and Global Climate program #DE-SC0016011. WRLA acknowledges funding from the David and Lucille Packard Foundation, NSF Dynamics of Coupled Natural and Human Systems #1714972, NSF Macrosystems #1802880, and the US Department of Agriculture National Institute of Food and Agriculture, Agricultural and Food Research Initiative Competitive Program, Ecosystem Services and Agro-ecosystem Management #2018-67019-27850.

ORCID

Steven A. Kannenberg https://orcid.org/0000-0002-4097-9140
Kimberly A. Novick https://orcid.org/0000-0002-8431-0879
M. Ross Alexander https://orcid.org/0000-0003-1106-1100
David J. P. Moore https://orcid.org/0000-0002-6462-3288
Richard P. Phillips https://orcid.org/0000-0002-1345-4138
William R. L. Anderegg https://orcid.org/0000-0001-6551-3331

REFERENCES

Alexander, M. R., Rollinson, C. R., Babst, F., Trouet, V., & Moore, D. J. P. (2018). Relative influences of multiple sources of uncertainty on cumulative and incremental tree-ring-derived aboveground biomass estimates. *Trees*, *32*(1), 265–276. https://doi.org/10.1007/s00468-017-1629-0

Anderegg, W. R. L., Martinez-Vilalta, J., Cailleret, M., Camarero, J. J., Ewers, B. E., Galbraith, D., … Trotsiuk, V. (2016). When a tree dies in the forest: Scaling climate-driven tree mortality to ecosystem water and carbon fluxes. *Ecosystems*, *19*(6), 1133–1147. https://doi.org/10.1007/s10021-016-9982-1

Anderegg, W. R. L., Plavcová, L., Anderegg, L. D. L., Hacke, U. G., Berry, J. A., & Field, C. B. (2013). Drought's legacy: Multiyear hydraulic deterioration underlies widespread aspen forest die-off and portends

increased future risk. *Global Change Biology*, *19*, 1188–1196. https://doi.org/10.1111/gcb.12100

Anderegg, W. R. L., Schwalm, C., Biondi, F., Camarero, J. J., Koch, G., Litvak, M., … Pacala, S. (2015). Pervasive drought legacies in forest ecosystems and their implications for carbon cycle models. *Science*, *349*(6247), 528–532. https://doi.org/10.1126/science.aab1833

Babst, F., Bodesheim, P., Charney, N., Friend, A. D., Girardin, M. P., Klesse, S., … Evans, M. E. K. (2018). When tree rings go global: Challenges and opportunities for retro- and prospective insight. *Quaternary Science Reviews*, *197*, 1–20. https://doi.org/10.1016/j.quascirev.2018.07.009

Bennett, A. C., McDowell, N. G., Allen, C. D., & Anderson-Teixeira, K. J. (2015). Larger trees suffer most during drought in forests worldwide. *Nature Plants*, *1*(10), 15139. https://doi.org/10.1038/nplants.2015.139

Berdanier, A. B., & Clark, J. S. (2016). Multi-year drought-induced morbidity preceding tree death in Southeastern US forests. *Ecology*, *26*(1), 17–23. https://doi.org/10.1890/15-0274

Bonan, G. B. (2008). Forests and climate change: Forcings, feedbacks, and the climate benefits of forests. *Science*, *320*, 1444–1449. https://doi.org/10.1126/science.1155121

Bréda, N., Huc, R., Granier, A., & Dreyer, E. (2006). Temperate forest trees and stands under severe drought: A review of ecophysiological responses, adaptation processes and long-term consequences. *Annals of Forest Science*, *63*(6), 625–644. https://doi.org/10.1051/forest:2006042

Brooks, J. R., Meinzer, F. C., Coulombe, R. O. B., & Gregg, J. (2002). Hydraulic redistribution of soil water during summer drought in two contrasting Pacific Northwest coniferous forests. *Tree Physiology*, *22*, 1107–1117. https://doi.org/10.1093/treephys/22.15-16.1107

Brzostek, E. R., Dragoni, D., Schmid, H. P., Rahman, A. F., Sims, D., Wayson, C. A., … Phillips, R. P. (2014). Chronic water stress reduces tree growth and the carbon sink of deciduous hardwood forests. *Global Change Biology*, *20*(8), 2531–2539. https://doi.org/10.1111/gcb.12528

Bunn, A. G. (2008). A dendrochronology program library in R (dplR). *Dendrochronologia*, *26*(2), 115–124. https://doi.org/10.1016/j.dendro.2008.01.002

Camarero, J. J., Gazol, A., Sangüesa-Barreda, G., Cantero, A., Sánchez-Salguero, R., Sánchez-Miranda, A., … Ibáñez, R. (2018). Forest growth responses to drought at short- and long-term scales in Spain: Squeezing the stress memory from tree rings. *Frontiers in Ecology and Evolution*, *6*. https://doi.org/10.3389/fevo.2018.00009

Campioli, M., Malhi, Y., Vicca, S., Luyssaert, S., Papale, D., Peñuelas, J., … Janssens, I. A. (2016). Evaluating the convergence between eddy-covariance and biometric methods for assessing carbon budgets of forests. *Nature Communications*, *7*, 13717. https://doi.org/10.1038/ncomms13717

Clark, J. S., Iverson, L., Woodall, C. W., Allen, C. D., Bell, D. M., Bragg, D. C., … Zimmermann, N. E. (2016). The impacts of increasing drought on forest dynamics, structure, and biodiversity in the United States. *Global Change Biology*, *22*(7), 2329–2352. https://doi.org/10.1111/gcb.13160

Colangelo, M., Camarero, J. J., Borghetti, M., Gazol, A., Gentilesca, T., & Ripullone, F. (2017). Size matters a lot: Drought-affected Italian oaks are smaller and show lower growth prior to tree death. *Frontiers in Plant Science*, *8*, 135. https://doi.org/10.3389/fpls.2017.00135

Cook, B. I., Ault, T. R., & Smerdon, J. E. (2015). Unprecedented 21st century drought risk in the American Southwest and Central Plains. *Science Advances*, *1*(1). https://doi.org/10.1126/sciadv.1400082

Cook, E. R. (1985). A time series analysis approach to tree ring standardization. PhD thesis, University of Arizona.

Cook, E. R., & Peters, K. (1981). The smoothing spline: A new approach to standardizing forest interior tree-ring width series for dendroclimatic studies. *Tree-Ring Bulletin*, *41*, 45–53.

Čufar, K., Prislan, P., De Luis, M., & Gričar, J. (2008). Tree-ring variation, wood formation and phenology of beech (*Fagus sylvatica*) from a representative site in Slovenia, SE Central Europe. *Trees*, *22*(6), 749–758. https://doi.org/10.1007/s00468-008-0235-6

D'Orangeville, L., Maxwell, J., Kneeshaw, D., Pederson, N., Duchesne, L., Logan, T., … Phillips, R. P. (2018). Drought timing and local climate determine the sensitivity of eastern temperate forests to drought. *Global Change Biology*, *24*(6), 2339–2351. https://doi.org/10.1111/gcb.14096

Dai, A. (2013). Increasing drought under global warming in observations and models. *Nature Climate Change*, *3*(1), 52–58. https://doi.org/10.1038/nclimate1633

Dai, A., Trenberth, K. E., & Qian, T. (2004). A global dataset of Palmer Drought Severity Index for 1870–2002: Relationship with soil moisture and effects of surface warming. *Journal of Hydrometeorology*, *5*(6), 1117–1130. https://doi.org/10.1175/jhm-386.1

Delpierre, N., Berveiller, D., Granda, E., & Dufr, E. (2016). Wood phenology, not carbon input, controls the interannual variability of wood growth in a temperate oak forest. *New Phytologist*, *210*(2), 459–470. https://doi.org/10.1111/nph.13771

DeRose, R. J., Shaw, J. D., & Long, J. N. (2017). Building the forest inventory and analysis tree-ring data set. *Journal of Forestry*, *115*(4), 283–291. https://doi.org/10.5849/jof.15-097

Doughty, C. E., Malhi, Y., Araujo-Murakami, A., Metcalfe, D. B., Silva-Espejo, J., Arroyo, L., … Ledezma, R. (2014). Allocation trade-offs dominate the response of tropical forest growth to seasonal and interannual drought. *Ecology*, *95*(8), 2192–2201. https://doi.org/10.1890/13-1507.1

Doughty, C. E., Metcalfe, D. B., Girardin, C. A. J., Amézquita, F. F., Cabrera, D. G., Huasco, W. H., … Malhi, Y. (2015). Drought impact on forest carbon dynamics and fluxes in Amazonia. *Nature*, *519*(7541), 78–82. https://doi.org/10.1038/nature14213

Dragoni, D., Schmid, H. P., Wayson, C. A., Potter, H., Grimmond, C. S. B., & Randolph, J. C. (2011). Evidence of increased net ecosystem productivity associated with a longer vegetated season in a deciduous forest in south-central Indiana, USA. *Global Change Biology*, *17*(2), 886–897. https://doi.org/10.1111/j.1365-2486.2010.02281.x

Dye, A., Alexander, M. R., Bishop, D., Druckenbrod, D., Pederson, N., & Hessl, A. (2018). Size–growth asymmetry is not consistently related to productivity across an eastern US temperate forest network. *Oecologia*, *189*(2), 1–14. https://doi.org/10.1007/s00442-018-4318-9

Dye, A., Plotkin, A. B., Bishop, D., Pederson, N., Poulter, B., & Hessl, A. (2016). Comparing tree-ring and permanent plot estimates of aboveground net primary production in three eastern U.S. forests. *Ecosphere*, *7*(9), e01454. https://doi.org/10.1002/ecs2.1454

Ehman, J. L., Schmid, H. P., Grimmond, C. S. B., Randolph, J. C., Hanson, P. J., Wayson, C. A., & Cropley, F. D. (2002). An initial intercomparison of micrometeorological and ecological inventory estimates of carbon exchange in a mid-latitude deciduous forest. *Global Change Biology*, *8*(6), 575–589. https://doi.org/10.1046/j.1365-2486.2002.00492.x

Elliott, K. J., Miniat, C. F., Pederson, N., & Laseter, S. H. (2015). Forest tree growth response to hydroclimate variability in the southern Appalachians. *Global Change Biology*, *21*(12), 4627–4641. https://doi.org/10.1111/gcb.13045

Evans, M. E. K., Falk, D. A., Arizpe, A., Swetnam, T. L., Babst, F., & Holsinger, K. E. (2017). Fusing tree-ring and forest inventory data to infer influences on tree growth. *Ecosphere*, *8*(7). https://doi.org/10.1002/ecs2.1889

Flexas, J., & Medrano, H. (2002). Drought-inhibition of photosynthesis in C3 plants: Stomatal and non-stomatal limitations revisited. *Annals of Botany*, *89*(2), 183–189. https://doi.org/10.1093/aob/mcf027

Fritts, H. C. (1976). *Tree rings and climate*. Cambridge, MA: Academic Press.

Galiano, L., Timofeeva, G., Saurer, M., Siegwolf, R., Martínez-Vilalta, J., Hommel, R., & Gessler, A. (2017). The fate of recently fixed carbon

after drought release : Towards unravelling C storage regulation in *Tilia platyphyllos* and *Pinus sylvestris*. *Plant, Cell & Environment*, *40*, 1711–1724. https://doi.org/10.1111/pce.12972

Gallé, A., Haldimann, P., & Feller, U. (2007). Photosynthetic performance and water relations in young pubescent oak (*Quercus pubescens*) trees during drought stress and recovery. *New Phytologist*, *174*, 799–810. https://doi.org/10.1111/j.1469-8137.2007.02047.x

Gazol, A., Camarero, J. J., Anderegg, W. R. L., & Vicente-Serrano, S. M. (2017). Impacts of droughts on the growth resilience of Northern Hemisphere forests. *Global Ecology and Biogeography*, *26*(2), 166–176. https://doi.org/10.1111/geb.12526

Gazol, A., Camarero, J. J., Vicente-Serrano, S. M., Sánchez-Salguero, R., Gutiérrez, E., de Luis, M., … Galván, J. D. (2018). Forest resilience to drought varies across biomes. *Global Change Biology*, *24*(5), 2143–2158. https://doi.org/10.1111/gcb.14082

Gessler, A., Schaub, M., & McDowell, N. G. (2016). The role of nutrients in drought-induced tree mortality and recovery. *New Phytologist*, 1443–1447. https://doi.org/10.1111/nph.14340

Giorgi, F., Im, E., Coppola, E., Diffenbaugh, N., Gao, X., Mariotti, L., & Shi, Y. (2011). Higher hydroclimatic intensity with global warming. *Journal of Climate*, *24*, 5309–5324. https://doi.org/10.1175/2011JCLI3979.1

Harris, I., Jones, P. D., Osborn, T. J., & Lister, D. H. (2014). Updated high-resolution grids of monthly climatic observations – the CRU TS3.10 Dataset. *International Journal of Climatology*, *34*(3), 623–642. https://doi.org/10.1002/joc.3711

Holmes, R. (1983). Computer-assisted quality control in tree-ring dating and measurement. *Tree-Ring Bulletin*, *43*, 69–78.

Kannenberg, S. A., Maxwell, J. T., Pederson, N., D'Orangeville, L., Ficklin, D. L., & Phillips, R. P. (2019). Drought legacies are dependent on water table depth, wood anatomy and drought timing across the eastern US. *Ecology Letters*, *22*(1), 119–127. https://doi.org/10.1111/ele.13173

Kannenberg, S. A., Novick, K. A., & Phillips, R. P. (2019). Anisohydric behavior linked to persistent hydraulic damage and delayed drought recovery across seven North American tree species. *New Phytologist*, *222*(4), 1862–1872. https://doi.org/10.1111/nph.15699

Klesse, S., DeRose, R. J., Guiterman, C. H., Lynch, A. M., O'Connor, C. D., Shaw, J. D., & Evans, M. E. K. (2018). Sampling bias overestimates climate change impacts on forest growth in the southwestern United States. *Nature Communications*, *9*(1), 5336. https://doi.org/10.1038/s41467-018-07800-y

Kolus, H. R., Huntzinger, D. N., Schwalm, C. R., Fisher, J. B., McKay, N., Fang, Y., … Shi, X. (2019). Land carbon models underestimate the severity and duration of drought's impact on plant productivity. *Scientific Reports*, *9*, 2758. https://doi.org/10.1038/s41598-019-39373-1

Landsberg, J., & Waring, R. (2016). Water relations in tree physiology: Where to from here? *Tree Physiology*, *37*, 18–32. https://doi.org/10.1093/treephys/tpw102

Lasslop, G., Reichstein, M., Papale, D., Richardson, A. D., Arneths, A., Barr, A., … Wohlfahrt, G. (2010). Separation of net ecosystem exchange into assimilation and respiration using a light response curve approach : Critical issues and global evaluation. *Global Change Biology*, *16*(1), 187–208. https://doi.org/10.1111/j.1365-2486.2009.02041.x

Lloret, F., Escudero, A., Iriondo, J. M., Martínez-Vilalta, J., & Valladares, F. (2012). Extreme climatic events and vegetation: The role of stabilizing processes. *Global Change Biology*, *18*(3), 797–805. https://doi.org/10.1111/j.1365-2486.2011.02624.x

Lutz, J. A., Furniss, T. J., Johnson, D. J., Davies, S. J., Allen, D., Alonso, A., … Zimmerman, J. K. (2018). Global importance of large-diameter trees. *Global Ecology and Biogeography*, *27*(7), 849–864. https://doi.org/10.1111/geb.12747

Mallya, G., Zhao, L., Song, X. C., Niyogi, D., & Govindaraju, R. S. (2013). 2012 Midwest drought in the United States. *Journal of Hydrologic Engineering*, *18*, 737–745. https://doi.org/10.1061/(ASCE)HE.1943-5584.0000786

Maxwell, J. T., Harley, G. L., & Robeson, S. M. (2016). On the declining relationship between tree growth and climate in the Midwest United States: The fading drought signal. *Climatic Change*, *138*(1), 127–142. https://doi.org/10.1007/s10584-016-1720-3

Mitchell, P. J., O'Grady, A. P., Tissue, D. T., Worledge, D., & Pinkard, E. A. (2014). Co-ordination of growth, gas exchange and hydraulics define the carbon safety margin in tree species with contrasting drought strategies. *Tree Physiology*, *34*(5), 443–458. https://doi.org/10.1093/treephys/tpu014

Mund, M., Kutsch, W. L., Wirth, C., Kahl, T., Knohl, A., Skomarkova, M. V., & Schulze, E. D. (2010). The influence of climate and fructification on the inter-annual variability of stem growth and net primary productivity in an old-growth, mixed beech forest. *Tree Physiology*, *30*(6), 689–704. https://doi.org/10.1093/treephys/tpq027

Nehrbass-Ahles, C., Babst, F., Klesse, S., Nötzli, M., Bouriaud, O., Neukom, R., … Frank, D. (2014). The influence of sampling design on tree-ring-based quantification of forest growth. *Global Change Biology*, *20*(9), 2867–2885. https://doi.org/10.1111/gcb.12599

Nepstad, D. C., Tohver, I. M., Ray, D., Moutinho, P., & Cardinot, G. (2007). Mortality of large trees and lianas following experimental drought in an Amazon forest. *Ecology*, *88*(9), 2259–2269. https://doi.org/10.1890/06-1046.1

Novick, K. A., Ficklin, D. L., Stoy, P. C., Williams, C. A., Bohrer, G., Oishi, A. C., … Phillips, R. P. (2016). The increasing importance of atmospheric demand for ecosystem water and carbon fluxes. *Nature Climate Change*, *6*, 1023–1027. https://doi.org/10.1038/nclimate3114

Oliveira, R. S., Dawson, T. E., Burgess, S. S. O., & Nepstad, D. C. (2005). Hydraulic redistribution in three Amazonian trees. *Oecologia*, *145*(3), 354–363. https://doi.org/10.1007/s00442-005-0108-2

Ouimette, A. P., Ollinger, S. V., Richardson, A. D., Hollinger, D. Y., Keenan, T. F., Lepine, L. C., & Vadeboncoeur, M. A. (2018). Carbon fluxes and interannual drivers in a temperate forest ecosystem assessed through comparison of top-down and bottom-up approaches. *Agricultural and Forest Meteorology*, *256–257*, 420–430. https://doi.org/10.1016/j.agrformet.2018.03.017

Pan, Y., Birdsey, R. A., Fang, J., Houghton, R., Kauppi, P. E., Kurz, W. A., … Hayes, D. (2011). A large and persistent carbon sink in the world's forests. *Science*, *333*, 988–993. https://doi.org/10.1126/science.1201609

Peltier, D. M. P., Fell, M., & Ogle, K. (2016). Legacy effects of drought in the southwestern United States: A multi-species synthesis. *Ecological Monographs*, *86*(3), 312–326. https://doi.org/10.1002/ecm.1219

Phillips, O. L., van der Heijden, G., Lewis, S. L., Lo, G., Lloyd, J., Malhi, Y., … Silva, J. (2010). Drought-mortality relationships for tropical forests. *New Phytologist*, *187*, 631–646.

Phillips, R. P., Ibáñez, I., D'Orangeville, L., Hanson, P. J., Ryan, M. G., & McDowell, N. G. (2016). A belowground perspective on the drought sensitivity of forests: Towards improved understanding and simulation. *Forest Ecology and Management*, *380*, 309–320. https://doi.org/10.1016/j.foreco.2016.08.043

Powell, T. L., Galbraith, D. R., Christoffersen, B. O., Harper, A., Imbuzeiro, H. M. A., Rowland, L., … Moorcroft, P. R. (2013). Confronting model predictions of carbon fluxes with measurements of Amazon forests subjected to experimental drought. *New Phytologist*, *200*(2), 350–365. https://doi.org/10.1111/nph.12390

Pretzsch, H., Schütze, G., & Uhl, E. (2013). Resistance of European tree species to drought stress in mixed versus pure forests: Evidence of stress release by inter-specific facilitation. *Plant Biology*, *15*(3), 483–495. https://doi.org/10.1111/j.1438-8677.2012.00670.x

Reichstein, M., Bahn, M., Ciais, P., Frank, D., Mahecha, M. D., Seneviratne, S. I., … Wattenbach, M. (2013). Climate extremes and the carbon cycle. *Nature*, *500*(7462), 287–295. https://doi.org/10.1038/nature12350

Richardson, A. D., Carbone, M. S., Keenan, T. F., Czimczik, C. I., Hollinger, D. Y., Murakami, P., … Xu, X. (2013). Seasonal dynamics and age of

stemwood nonstructural carbohydrates in temperate forest trees. *New Phytologist*, *197*(3), 850–861. https://doi.org/10.1111/nph.12042

Rocha, A. V., Goulden, M. L., Dunn, A. L., & Wofsy, S. C. (2006). On linking interannual tree ring variability with observations of whole-forest CO_2 flux. *Global Change Biology*, *12*(8), 1378–1389. https://doi.org/10.1111/j.1365-2486.2006.01179.x

Rollinson, C. R., Liu, Y., Raiho, A., Moore, D. J. P., McLachlan, J., Bishop, D. A., … Dietze, M. C. (2017). Emergent climate and CO_2 sensitivities of net primary productivity in ecosystem models do not agree with empirical data in temperate forests of eastern North America. *Global Change Biology*, *23*(7), 2755–2767. https://doi.org/10.1111/gcb.13626

Roman, D. T., Novick, K. A., Brzostek, E. R., Dragoni, D., Rahman, F., & Phillips, R. P. (2015). The role of isohydric and anisohydric species in determining ecosystem-scale response to severe drought. *Oecologia*, *179*(3), 641–654. https://doi.org/10.1007/s00442-015-3380-9

Rowland, L., Costa, A. C. L., Galbraith, D. R., Oliveira, R. S., Binks, O. J., Oliveira, A. A. R., … Meir, P. (2015). Death from drought in tropical forests is triggered by hydraulics not carbon starvation. *Nature*, *528*(7580), 119–122. https://doi.org/10.1038/nature15539

Rowland, L., da Costa, A. C. L., Oliveira, A. A. R., Oliveira, R. S., Bittencourt, P. L., Costa, P. B., … Meir, P. (2018). Drought stress and tree size determine stem CO_2 efflux in a tropical forest. *New Phytologist*, *218*, 1393–1405. https://doi.org/10.1111/nph.15024

Sala, A., Woodruff, D. R., & Meinzer, F. C. (2012). Carbon dynamics in trees: Feast or famine? *Tree Physiology*, *32*(6), 764–775. https://doi.org/10.1093/treephys/tpr143

Schimel, J., Balser, T. C., & Wallenstein, M. (2007). Microbial stress-response physiology and its implications for ecosystem function. *Ecology*, *88*(6), 1386–1394. https://doi.org/10.1890/06-0219

Schmid, H. P., Grimmond, C. S. B., Cropley, F., Offerle, B., & Su, H. (2000). Measurements of CO_2 and energy fluxes over a mixed hardwood forest in the mid-western United States. *Agricultural and Forest Meterology*, *103*, 357–374. https://doi.org/10.1016/s0168-1923(00)00140-4

Schwalm, C. R., Anderegg, W. R. L., Michalak, A. M., Fisher, J. B., Biondi, F., Koch, G., … Tian, H. (2017). Global patterns of drought recovery. *Nature*, *548*, 202–205. https://doi.org/10.1038/nature23021

Seftigen, K., Frank, D. C., Björklund, J., Babst, F., & Poulter, B. (2018). The climatic drivers of normalized difference vegetation index and tree-ring-based estimates of forest productivity are spatially coherent but temporally decoupled in Northern Hemispheric forests. *Global Ecology and Biogeography*, *27*(11), 1352–1365. https://doi.org/10.1111/geb.12802

Skomarkova, M. V., Vaganov, E. A., Mund, M., Knohl, A., Linke, P., Boerner, A., & Schulze, E. D. (2006). Inter-annual and seasonal variability of radial growth, wood density and carbon isotope ratios in tree rings of beech (*Fagus sylvatica*) growing in Germany and Italy. *Trees—Structure and Function*, *20*(5), 571–586. https://doi.org/10.1007/s00468-006-0072-4

Stephenson, N. L., Das, A. J., Ampersee, N. J., Bulaon, B. M., & Yee, J. L. (2019). Which trees die during drought? The key role of insect host-tree selection. *Journal of Ecology*. https://doi.org/10.1111/1365-2745.13176

Stocker, B. D., Zscheischler, J., Keenan, T. F., Prentice, I. C., Peñuelas, J., & Seneviratne, S. I. (2018). Quantifying soil moisture impacts on light use efficiency across biomes. *New Phytologist*, *218*(4), 1430–1449. https://doi.org/10.1111/nph.15123

Stocker, B. D., Zscheischler, J., Keenan, T. F., Prentice, I. C., Seneviratne, S. I., & Peñuelas, J. (2019). Drought impacts on terrestrial productions underestimated by satellite monitoring. *Nature Geoscience*, *12*, 264–270. https://doi.org/10.1038/s41561-019-0318-6

Stokes, M. A., & Smiley, T. L. (1999). *An introduction to tree-ring dating*. Tucson, AZ: University of Arizona Press.

Sulman, B. N., Roman, D. T., Scanlon, T. M., Wang, L., & Novick, K. A. (2016). Comparing methods for partitioning a decade of carbon dioxide and water vapor fluxes in a temperate forest. *Agricultural and Forest Meteorology*, *226*, 229–245. https://doi.org/10.1016/j.agrformet.2016.06.002

Teets, A., Fraver, S., Hollinger, D. Y., Weiskittel, A. R., Seymour, R. S., & Richardson, A. D. (2017). Linking annual tree growth with eddy-flux measures of net ecosystem productivity across twenty years of observation in a mixed conifer forest. *Agricultural and Forest Meteorology*, *249*, 479–487. https://doi.org/10.1016/j.agrformet.2017.08.007

Trugman, A. T., Detto, M., Bartlett, M. K., Medvigy, D., Anderegg, W. R. L., Schwalm, C., … Pacala, S. W. (2018). Tree carbon allocation explains forest drought-kill and recovery patterns. *Ecology Letters*, *21*(10), 1552–1560. https://doi.org/10.1111/ele.13136

Tuck, S., Phillips, H., Hintzen, R., Scharlemann, J., Purvis, A., & Hudson, L. (2014). MODISTools—Downloading and processing MODIS remotely sensed data in R. *Ecology and Evolution*, *4*(24), 4658–4668. https://doi.org/10.1002/ece3.1273

van der Molen, M. K., Dolman, A. J., Ciais, P., Eglin, T., Gobron, N., Law, B. E., … Wang, G. (2011). Drought and ecosystem carbon cycling. *Agricultural and Forest Meteorology*, *151*(7), 765–773. https://doi.org/10.1016/j.agrformet.2011.01.018

van Gorsel, E., Delpierre, N., Leuning, R., Black, A., Munger, J. W., Wofsy, S., … Wharton, S. (2009). Estimating nocturnal ecosystem respiration from the vertical turbulent flux and change in storage of CO_2. *Agricultural and Forest Meteorology*, *149*(11), 1919–1930. https://doi.org/10.1016/j.agrformet.2009.06.020

Vose, J. M., Clark, J. S., Luce, C. H., & Patel-Weynand, T. (2016). Effects of drought on forests and rangelands in the United States: A comprehensive science synthesis. U.S. Dept of Agriculture General Technical Report, WO-93a, 302.

Wu, X., Liu, H., Li, X., Ciais, P., Babst, F., Guo, W., … Ma, Y. (2017). Differentiating drought legacy effects on vegetation growth over the temperate Northern hemisphere. *Global Change Biology*, *24*(1), 504–516. https://doi.org/10.1111/gcb.13920

Xu, K., Wang, X., Liang, P., An, H., Sun, H., Han, W., & Li, Q. (2017). Tree-ring widths are good proxies of annual variation in forest productivity in temperate forests. *Scientific Reports*, *7*, 1945. https://doi.org/10.1038/s41598-017-02022-6

Yamaguchi, D. (1991). A simple method for cross-dating increment cores from living trees. *Canadian Journal of Forest Research*, *21*, 414–416. https://doi.org/10.1139/x91-053

Yi, K., Dragoni, D., Phillips, R. P., Roman, D. T., & Novick, K. A. (2017). Dynamics of stem water uptake among isohydric and anisohydric species experiencing a severe drought. *Tree Physiology*, *37*(10), 1379–1392. https://doi.org/10.1093/treephys/tpx014

Yi, K., Maxwell, J. T., Wenzel, M. K., Roman, D. T., Sauer, P. E., Phillips, R. P., & Novick, K. A. (2019). Linking variation in intrinsic water-use efficiency to isohydricity: A comparison at multiple spatiotemporal scales. *New Phytologist*, *221*(1), 195–208. https://doi.org/10.1111/nph.15384

Zimmerman, M. (1983). *Xylem structure and the ascent of sap*. Berlin, Germany: Springer-Verlag.

SUPPORTING INFORMATION

Additional supporting information may be found online in the Supporting Information section at the end of the article.

How to cite this article: Kannenberg SA, Novick KA, Alexander MR, et al. Linking drought legacy effects across scales: From leaves to tree rings to ecosystems. *Glob Change Biol*. 2019;25:2978–2992. https://doi.org/10.1111/gcb.14710